Residual Stresses and Strength of Hard Chromium Coatings

Wulf Pfeiffer, Christof Koplin, E. Reisacher, J. Wenzel

Fraunhofer Institute for Mechanics of Materials IWM, Woehlerstr. 11, 79108 Freiburg, Germany

wulf.pfeiffer@iwm.fraunhofer.de, christof.koplin@iwm.fraunhofer.de,
eduard.reisacher@iwm.fraunhofer.de, Johannes.wenzel@iwm.fraunhofer.de

Keywords: hard chromium, plating, residual stress, cracks, strength.

Abstract. Experimental and numerical investigations have been performed on the relationships between coating parameters, residual stresses, micro-cracks and the near surface strength of hard chromium coatings. The experimental investigations included: X-ray measurements of residual and externally-applied stresses; crack density measurements using microscopy; and load-bearing measurements using ball-on-plate tests. The numerical investigations in combination with analytical conclusions focused on the influence of different crack lengths and densities on the effective elastic modulus of the chromium coating and the stress-enhancing or shielding effect of micro-crack networks respectively. The results show that the residual stresses and crack networks are influenced by the current density used during deposition. Coatings with high tensile residual stresses have low crack densities. This correlation is associated with stress relaxation by formation of micro-cracks and, to a lesser extent, to a direct reduction in residual stresses due to the deposition process. The load bearing capacity is dominated by the crack density and can be significantly increased by shot-peening-induced compressive residual stresses. Thus, optimization of hard chromium deposition parameters for applications needing high surface strength should predominantly focus on minimizing the crack density.

Introduction

Hard chromium coatings, deposited by electroplating, are well established coatings in wear applications. The thicknesses of the coatings can range from several hundred microns (e.g. in feed pipes for abrasive slurries) to only a few microns (e.g. for high pressure injector valve seats). In any case, the performance of hard chromium coatings is limited by the development of micro cracks and tensile residual stresses during deposition. Thus, optimization of deposition parameters should account for the structural integrity of the coatings in addition to economic factors.

The purpose of this study was to:

(i) establish correlations between the current density, crack density and residual stresses,
(ii) clarify the role of micro cracks in the development of residual stresses
(iii) develop a methodology for improving the structural integrity of hard chromium coatings.

Experimental details

Coating. Electroplating of steel discs (diameter 25 mm, thickness 8 mm), which were machined from the steel 1.7225 in quenched and tempered condition, was performed in a flow-through reactor using sulfuric acid electrolyte at 55°C and current densities ranging from 30 up to 90 A/dm^2. About 20 differently coated specimens were investigated. For bending experiments, strips with dimensions 100 mm x 20 mm x 2 mm were coated under similar conditions in a separate reactor. The thicknesses of the coatings were around 150 µm.

Crack density. The crack densities were evaluated from SEM micrographs by counting the number of intersections between cracks and a ~200 µm line drawn parallel to the coating's surface,

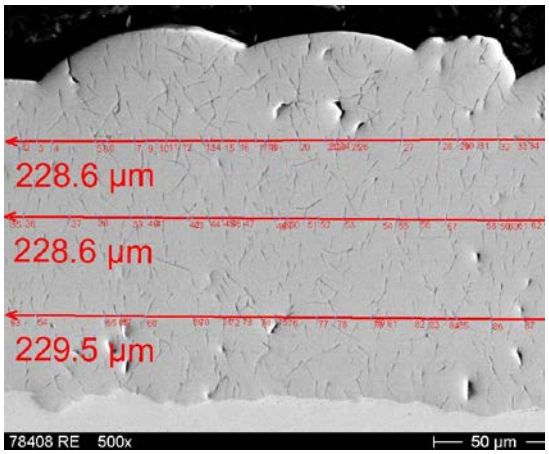

Fig. 1: Micrograph (SEM) of a hard chromium coating with numbering of intersections of lines with micro cracks.

see Fig. 1. The near-surface crack densities were calculated using the line at 75% of the coating thickness.

X-ray stress measurement. X-ray residual stress measurements were performed using CrKα-radiation (penetration depth approximately 5 µm) and the {211} lattice planes of chromium. Typically 15 peak positions were determined at ψ-tilts up to ±70°. In contrast to the textured-appearance of hard chromium coatings reported in the literature [4], the coatings investigated here showed no significant texture and the resulting $\sin^2\psi$-distributions were linear. Thus, stresses could be calculated using the classical $\sin^2\psi$-method [1] using X-ray elastic constants (XEC) calculated from the single crystal coefficients using the Kröner model [2], [3]. For loading stress measurements, a fully automated 4-point bending device was used, with the distances between the loading supports being 20 mm. The applied loads were calculated from the readings of the load and the geometrical conditions. To avoid the influence of plastic deformation and/or crack growth, all investigations were performed during the unloading cycle.

Load bearing capacity. The static load bearing capacity was determined using ball-indentation tests. The advantage of this testing method is its high surface sensitivity due to the rapidly decreasing tensile stresses with depth. Thus, the "surface strength" of a brittle material can be quantified using this test. The tests were performed using an electro-mechanical testing machine. The load carrying capacity was determined by a continuous increase of the load until an acoustic sensor detects sound emitted by a damage-event. The diameter of the indenter was 11.1 mm. Due to the roughness of the sample surfaces, a mechanical polishing process was applied before testing. This also flattened the residual stress states of the near surface regions. Thus, the results of these tests are mainly related to the crack networks.

Results

Influence of current density on the residual stress. As an example, Fig. 2 shows near surface residual stresses of specimens coated with constant current densities of between 30 A/dm² and

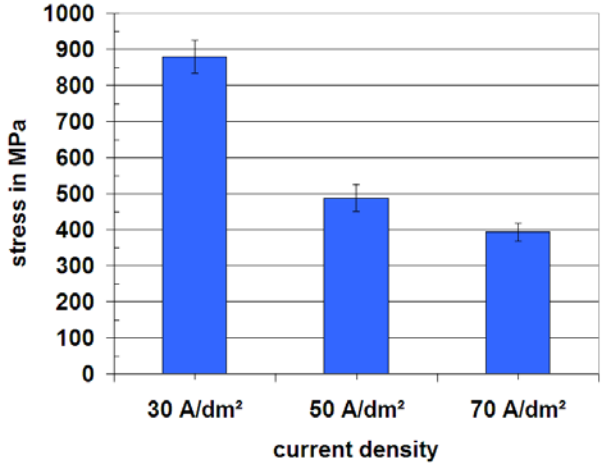

Fig. 2: Dependency of surface residual stresses of coatings deposited using constant current densities.

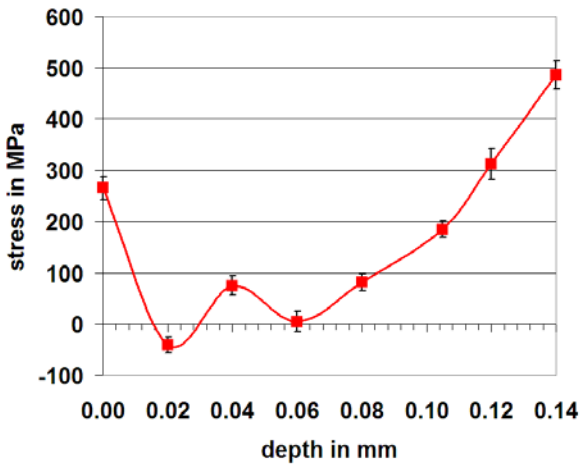

Fig. 3: Depth distribution of residual stresses in a coating deposited using a current density increasing from 30 to 90 A/dm².

70 A/dm^2. There is a clear tendency towards decreasing tensile residual stresses with increasing current density.

The increase in residual stresses with current density was also reflected in distribution with respect to depth of residual stresses in coatings deposited using a steadily increasing current density. The coating shown in Fig. 3 was deposited using an increasing current density from 30 A/dm^2 up to 90 A/dm^2 (Fig. 3). In the near surface region (< 0.02 mm) the residual stresses are increasing with decreasing depth (i.e. current density). This may be related to the effect of higher oxygen concentrations in the near surface layer of coatings, reported by [5].

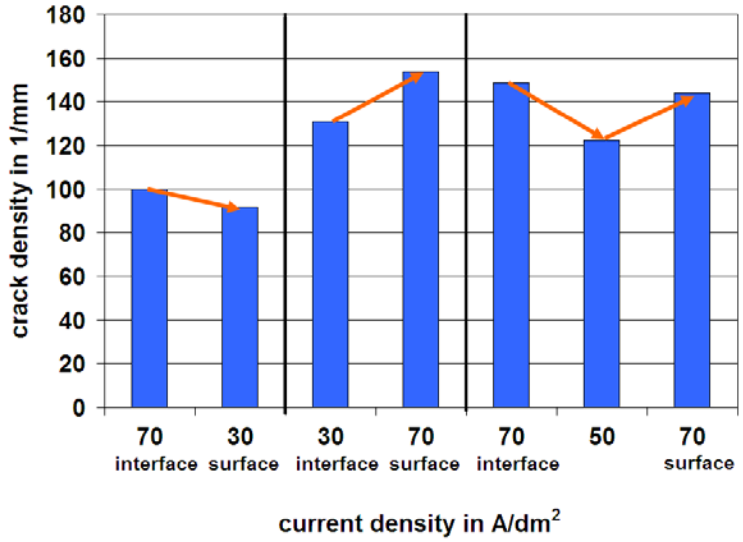

Fig. 4: Crack densities at 25%, (50%) and 75% height of coatings deposited in two (three) layers using different current densities.

Influence of current density on the crack density. Fig. 4 shows crack densities for coatings deposited using a stepwise or alternating current density. The crack densities were measured at 25% and 75% of the coating thickness in case of dual-layered coatings and additionally at 50% of the coating thickness in the case of triple-layered coatings. In all cases there is a decrease in crack density with decreasing current density. The crack density is also dependent on the position of the investigated layer within the dual and triple-layered coatings.

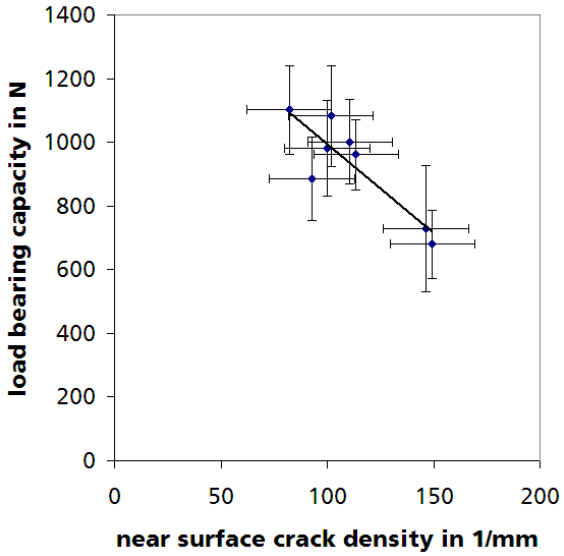

Fig. 5: Correlation between the load bearing capacity and the near surface crack density.

Influence of the crack density on the load bearing capacity. Mechanical polishing of the ball indentation specimen surfaces resulted in superimposed residual stresses. Thus, only the influence of different crack densities on the load bearing capacity could be studied. Fig. 5 shows the effect of the crack density on the load bearing capacity of coatings deposited using a variety of deposition parameters. The increase in crack density corresponds with a decrease in the load bearing of the chromium layers.

Discussion

Influence of the crack density on the residual stress determination. The characterization of the strength of materials containing micro-crack networks using X-ray residual stress measurements is generally not straight forward. For determining the macroscopic constraint between the coating and the substrate, the X-ray elastic constants (XEC) determined using loading experiments can be used. For determining the stresses within the intact sub-volumes of the coating, the XEC of a homogeneous chromium material should be used. Since electroplated chromium with sufficient thickness for experimental XEC determination will always contain micro-cracks, the influence of cracks on the elastic constants can be eliminated by introducing high compressive residual stresses

(> 1 GPa) through a newly developed shot peening process for brittle materials [6]. The XEC calculated from the single crystal coefficients are compared with the XEC of coatings with micro cracks and coatings with closed micro cracks in Table 1. The difference between the calculated XEC and the measured XEC of the coating with closed micro cracks may be attributed to the influence of the thick steel substrate which dominates the development of strains in the coating the during mechanical loading.

Table 1: XEC ((ν+1)/E) calculated from the single crystal coefficients and experimentally determined on coatings with micro cracks and coatings with closed micro cracks [1/GPa].

calculated	closed micro cracks	70 micro cracks / mm
3.57	3.20 ± 0.08	2.92 ± 0.2

The difference between the XEC of the coatings with open and closed cracks is small. Thus, it can be concluded that the differing crack densities of the investigated specimens have no significant influence on the amount of residual stresses.

Influence of the stress relaxation effect on the residual stress development. The correlation of the decreasing residual stress with the increasing crack density is based on the assumption of an intrinsic residual stress, i.e. the stress that would be measured if material strength is sufficient such that no cracking occurs, and that the hypothetical intrinsic residual stress is not affected by crack formation. Therefore, the actual resulting residual stress can be calculated from the stress relieving effect by calculation of an effective elastic modulus [7]. In this case, the effective elastic modulus depends on the density of tunnel cracks of length *a* in 2-dimensions. Consequently, the measured one dimensional crack density ρ can be used to derive a relative 2-dimensional crack density φ (1). The effective modulus E_{eff} thus leads to a strain relaxation ε_{relax}, that can be quantified by $S = E_{eff}/E$ (2).

$$\varphi = \frac{a^2}{\pi\left(a+\frac{1}{2\rho}\right)\frac{1}{2\rho}} \quad . \tag{1}$$

$$\sigma_{residual,\,eff}/E = \varepsilon - \varepsilon_{relax} = S\cdot\varepsilon = S\cdot\sigma_{residual,intrinsic}/E \quad . \tag{2}$$

Using this approach, one can fit the model with surface residual stress against near surface crack density. As a result, crack length and intrinsic residual stress could be adapted, Table 2. Fig. 6 shows, that the stress relieving effect of micro cracks can't describe the development of residual stresses satisfactorily.

Table 2: Resulting crack length and intrinsic residual stress of the adapted self-consistent model of micro-cracked solids.

crack length [µm]	Intrinsic residual stress [MPa]
17	1044

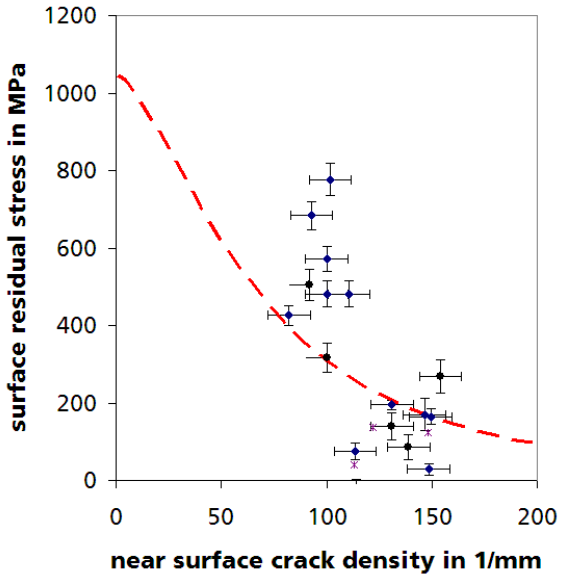

Fig. 6: Fit of the residual stress releasing effect of micro cracks using a self-consistent model for micro-cracked solids.

Modeling of the effect of micro-crack networks on the load bearing capacity. From numerical simulations (not presented here) it could be concluded that an effective elastic modulus (as discussed above) has only a limited influence on the maximal tensile stress, even for the highest crack densities. The coating was modeled using a Youngs modulus of E = 350 GPa (in case of compressive stresses), assumed values of E_{eff} in case of tensile stresses and E = 220 GPa for the substrate. The geometrical setup was the same as for the ball-indentation tests (with the indenter having E = 200 GPa). The coating thickness was assumed to be 150 µm. The maximal principal stresses were calculated with or without a deterministic surface crack (length 10µm, crack tip diameter 1µm).

For a deterministic crack E_{eff} = 0.5 * E would increase the crack tip stress by only 10%. In the case of no deterministic crack the surface stress would be reduced by 10%. Nevertheless, the micro crack network has a significant influence due to the near field crack interaction:

For a decrease of load bearing capacity, both an increasing crack density and a special geometrical arrangement of cracks (Fig. 7) is needed. FEM investigations (not shown here) of parallel aligned cracks oriented perpendicular to the stress axis showed a stress shielding effect. Stress shielding would be accompanied with an increase of load bearing capacity with increasing crack density. In contrast to the stress shielding of aligned cracks the decrease on load bearing capacity could be explained by the superposition of stress fields of non-parallel aligned interacting cracks (Fig. 8).

For those cracks an approximation function *V* (3) of the resulting K_I factor is given by [1]. The following assumption for the geometrical parameter was made (4).

$$K_I = V(2a/d, e/f) \cdot \sigma_{rr}^{max} \sqrt{\pi \cdot a} \,. \tag{3}$$

$$e/f = \frac{1}{2}(a \cdot \rho + 1), \qquad d = \sqrt{\frac{1}{\rho^2} + \frac{1}{4}\left(a + \frac{1}{\rho}\right)^2} \,. \tag{4}$$

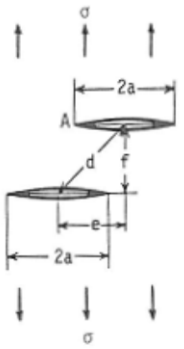

Fig. 7: The geometrical parameters for the approximation of K_I for cracks with a parallel offset.

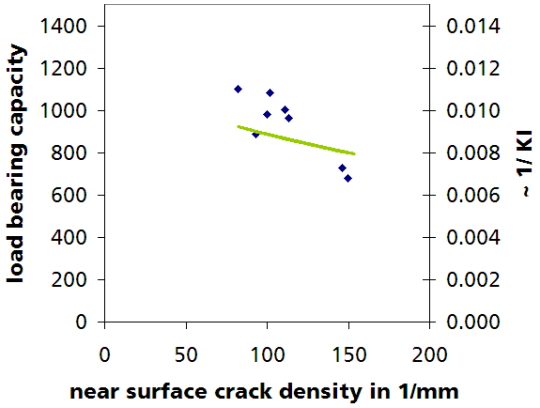

Fig. 8: The load bearing capacity of the ball indentation test and the reciprocal K_I for cracks with parallel offset.

The increase of K_I of a deterministic crack with increasing crack density (Fig. 9) could partially explain the reduction of the load bearing capacity. Since the observed crack morphology is statistically distributed with respect to the length, alignment and spatial distribution of cracks, the comparison is rough. The statistical effects could increase the effect of near field interaction further [9].

Conclusions

In general, electroplating of hard chromium on steel results in coatings with tensile residual stresses and crack networks. Using appropriate current densities it is possible to minimize tensile residual stress and crack densities – but not concurrently. The amount of residual stress is inversely proportional to the crack density. However, calculations show that the stress relaxation effect of the micro-cracks is not the only stress-determining mechanism. The near surface strength (load bearing capacity) is dominated by the crack density. The effect of the micro-cracks on the load bearing capacity can be described by analytical expressions that include the effect of both the crack density and the spatial distribution of cracks. To correctly describe the decrease of the load bearing capacity with an increasing crack density it is necessary that the cracks are not arranged in a parallel way. Due to the need for mechanical surface preparation, the effect of the residual stresses on the load bearing capacity could not be determined in this investigation. Nevertheless, from investigations into shot peening induced compressive residual stresses it has been shown that residual stresses can have a dramatic effect on the strength of hard chromium coatings [6].

Acknowledgements

These investigations were sponsored by the Bundesministeriums für Bildung und Forschung under contract number 01Rl 05273. Electroplating was performed by the Fraunhofer Institute for Manufacturing Engineering and Automation IPA, Stuttgart, Germany.

References

[1] P. Müller, E. Macherauch: Z. ang. Phys. 13 (1961), pp. 305-312.

[2] Landolt-Börnstein, Gruppe III, Band 11, Springer Verlag, Berlin/Heidelberg/New York (1979).

[3] Hans Uwe Baron, Viktor Hauk: Zeitschrift Metallkunde Bd. 79 (1988), pp. 127-131.

[4] J. Pina et al., in: *Surface and Coatings Technology* Vol. 96 (1997), pp. 148-162.

[5] V. Cassagne et al., in: *Proc. of ICRS-5*, Vol 2 (1997), 1042-1047, Linköping University, Sweden.

[6] W. Pfeiffer et al.: Materials Science Forum Vols. 638-642 (2010), pp799-804. Trans Tech Publ., Switzerland.

[7] Y Huang, K X Hu, A Chandra: J. of Mech. Phys. Solids 42(8) (1994), pp. 1273-1291.

[8] Stress intensity factors handbook (1), Pergamon Press (1987).

[9] A. Carpinter, C. Scavia: Fracture Processes in Concrete, Rock and Ceramics RILEM , London (1991) 173-182.